

Modification of silicophosphate glass composition, structure, and properties via crucible material and melting conditions





Nuttawan Sawangboon, Alina Nizamutdinova, Tobias Uesbeck, René Limbach, Ekarat Meechoowas, Kanit Tapasa, Doris Möncke, Lothar Wondraczek, Efstratios I. Kamitsos, Leo van Wüllen, Delia S. Brauer

Angaben zur Veröffentlichung / Publication details:

Sawangboon, Nuttawan, Alina Nizamutdinova, Tobias Uesbeck, René Limbach, Ekarat Meechoowas, Kanit Tapasa, Doris Möncke, et al. 2019. "Modification of silicophosphate glass composition, structure, and properties via crucible material and melting conditions." *International Journal of Applied Glass Science* 11 (1): 46–57.
<https://doi.org/10.1111/ijag.13958>.

SPECIAL ISSUE ARTICLE

Modification of silicophosphate glass composition, structure, and properties via crucible material and melting conditions

Nuttawan Sawangboon¹ | Alina Nizamutdinova² | Tobias Uesbeck² | René Limbach¹ |
Ekarat Meechoowas³ | Kanit Tapasa³ | Doris Möncke^{1,4,5}  | Lothar Wondraczek¹  |
Efstratios I. Kamitsos⁴  | Leo van Wüllen² | Delia S. Brauer¹ 

¹Otto Schott Institute of Materials
Research, Friedrich Schiller University
Jena, Jena, Germany

²Institute of Physics, Augsburg University,
Augsburg, Germany

³Thailand Center of Excellence for
Glass, Department of Science Service,
Bangkok, Thailand

⁴Theoretical and Physical Chemistry
Institute, National Hellenic Research
Foundation, Athens, Greece

⁵Inamori School of Engineering at the New
York State College of Ceramics, Alfred
University, Alfred, NY, USA

Correspondence

Delia S. Brauer, Otto Schott Institute of
Materials Research, Friedrich Schiller
University Jena, Fraunhoferstr. 6, Jena
07743, Germany.

Email: delia.brauer@uni-jena.de

Funding information

Deutsche Forschungsgemeinschaft, Grant/
Award Number: BR 4608/5 (SPP 1594);
Ministry of Science and Technology of
Thailand

Abstract

Ceramic crucibles are known to corrode in contact with glass melts. Here, we investigate the effect of alumina and fused silica crucibles on the composition, structure, and properties of silicophosphate glasses. Glasses in the system $0.3 \text{ Na}_2\text{O}-0.6 \text{ P}_2\text{O}_5-0.1 \text{ SiO}_2$ were melted in platinum, alumina, or fused silica crucibles at 900°C or 1200°C for 0.5–12 hours. Al_2O_3 and SiO_2 were found to leach from the crucibles into the glass melt and alter the glass composition: Al_2O_3 content increased with melting temperature and time, resulting in up to 10 mol% Al_2O_3 ; SiO_2 from fused silica crucibles was also introduced into the glass, resulting in a 25% higher SiO_2 content compared to the nominal composition. Glass density, transition temperature, thermal expansion, and mechanical properties were strongly affected by these compositional changes. Based on vibrational spectroscopy, this is explained by increasing numbers of P–O–Al or P–O–Si bonds, resulting in a depolymerization of the phosphate network, and ionic cross-linking by high field strength aluminum or silicon ions. With increasing alumina content, P–O–Si bonds were replaced by P–O–Al bonds. ^{31}P and ^{27}Al MAS NMR spectra revealed that aluminum is present in sixfold coordination exclusively and fully bonded to phosphate species, connecting phosphate groups by P–O–Al–O–P bonds.

KEYWORDS

crucible material, IR spectroscopy, Raman spectroscopy, silicophosphate glass, sixfold-coordinated Si, solid-state NMR spectroscopy

1 | INTRODUCTION

High phosphate content silicophosphate glasses are known for the presence of sixfold-coordinated silicon even when prepared at ambient pressure.^{1–12} They are of potential interest for various applications, for example, optical fibers^{13,14} or in fuel cells.^{14,15} However, owing to their low chemical durability their use is still limited. The addition of Al_2O_3

to phosphate glasses not only affects the glass structure but also promotes chemical durability and improves the resistance to moisture invasion,^{16–21} and the effect of Al^{3+} ions has been described as strengthening the glass.²² In general, Al_2O_3 can be introduced into the glass network (a) by direct addition of either alumina to the batch or through adding other aluminous materials which require less energy and, thus, a lower temperature for melting, for example, $\text{Al}(\text{OH})_3$

TABLE 1 Silicophosphate (0.3 Na₂O-0.6 P₂O₅-0.1 SiO₂) glass melting conditions

Melting temperature (°C)	Crucible material	Melting time (h)	Sample name
900	Platinum	1	900Pt1
	Alumina	1	900A11
		3	900A13
		6	900A16
		12	900A112
1200	Fused silica	0.5	1200Si0.5
	Alumina	1	1200A11
		6	1200A16
		12	1200A112

or AlO(OH),^{23,24} or (b) by diffusion from alumina crucibles owing to crucible corrosion by the glass melt.^{25–30} In the latter case, the amount of dissolved Al³⁺ and O^{2–} depends on the melting conditions and the type of alumina crucible used. Our previous study showed that sixfold-coordinated silicon in these glasses is replaced by alumina and transforms into fourfold-coordinated silicon instead.³¹ The aim of this study was therefore to further characterize the structural effects of alumina on silicophosphate glasses while also investigating how alumina incorporation affects the glasses' thermal and mechanical properties. We were also interested to see whether diffusion of Al³⁺ from alumina crucibles can be used to systematically tailor glass properties. This is even more important since platinum crucibles are often damaged during melting of phosphate glass batches, owing to severe corrosion of the platinum metal.³² We therefore systematically studied the influence of crucible material and melting conditions on glass composition, structure, and properties of silicophosphate glasses.

2 | MATERIALS AND METHODS

2.1 | Glass synthesis

A series of glasses in the system 0.3 Na₂O-0.6 P₂O₅-0.1 SiO₂ (molar ratio) was prepared by a conventional melt-quench route. High-purity reagents (NaPO₃)_n (Sigma-Aldrich), NH₄H₂PO₄ (Carl Roth), and SiO₂ (Carl Roth) were used as batch materials. The powders were weighed for a batch size of 50 g and mixed for 10 minutes to obtain homogeneous batches. Subsequently, the batches were transferred to either a platinum, alumina (Ceramtrade GbR), or fused silica crucible (Qsil). The batches were preheated to 600°C for 30 minutes in an electrical furnace to ensure the removal of water, carbon dioxide, and ammonia. The batches were then melted at either 900°C or 1200°C for time periods between 0.5 and

12 hours. Melting conditions are summarized in Table 1. Afterwards, the melt was rapidly quenched between brass plates to room temperature, annealed near the glass transition temperature for 1 hour and cooled to room temperature inside the annealing oven over night (cooling rate ca. 30 K hour^{–1}). All samples were stored in a desiccator to avoid reaction with atmospheric humidity. The samples were cut into discs (thickness about 2 mm) and polished for analysis of chemical composition and spectroscopic measurements.

To facilitate the acquisition of NMR spectra and decrease relaxation times in REAPDOR (rotational echo adiabatic passage double resonance)^{33–35} experiments, an additional glass sample with a nominal composition of 97(0.3 Na₂O-0.6 P₂O₅-0.1 SiO₂)-3Al₂O₃ containing 0.01 wt% MnO (added as MnCO₃, to shorten the T₁-relaxation times) was prepared by melting in a platinum crucible at 1200°C for 1 hour.

2.2 | Glass characterization

The amorphous nature of the glasses was confirmed by X-ray powder diffraction (XRD; MiniFlex, Rigaku). Glass transition temperature (T_g), dilatometric softening point (T_s), and the coefficient of thermal expansion (α) of glass rods with a diameter of 5 mm and a length of 20 mm were determined by dilatometry (Netzsch DIL 402 PC, Netzsch GmbH) at a heating rate of 5 K minute^{–1}. The α values of the glasses were determined by linear fitting of the slope of dilatometry curves between 100°C and 300°C (glasses melted at 1200°C) or between 50°C and 200°C (glasses melted at 900°C, owing to their lower T_g). Error limits were ± 5 K for T_g and T_s and ± 0.1 × 10^{–6} K^{–1} for α. Glass density (ρ) was measured on monoliths using helium pycnometry (AccuPyc 1330, Micromeritics GmbH); the estimated error limit was 0.01 g cm^{–3}.

2.3 | Compositional analysis

Scanning electron microscopy (SEM; JSM 7001F, Jeol GmbH) with energy dispersive X-ray analysis (EDX; Trident Analysis System, EDAX Inc) was performed at 15 keV in order to analyze the actual composition of the glass samples (on two separate locations) and of the various alumina crucibles. The composition of the glass melted in a platinum crucible was analyzed by inductively coupled plasma optical emission spectroscopy (ICP-OES; Varian Liberty 150, Agilent Technologies). For this, 50 mg of fine powder (<38 μm) were digested in acidified water (20 mL of deionized water and 10 mL of 65% nitric acid, Suprapur grade, Merck) in a 50 mL volumetric flask inside an ultrasound bath (Sonorex super RK255H, Bandelin Electronic GmbH) until the glass was dissolved completely. Then the volumetric flask was filled with deionized water to 50 mL and the solution analyzed using ICP-OES (Varian Liberty 150, Agilent Technologies). Analyses were performed in triplicate.

TABLE 2 Actual composition (mol%) of 0.3 Na₂O-0.6 P₂O₅-0.1 SiO₂ glasses melted between 0.5 and 12 h

Sample name	Melting temp. (°C)	Crucible material	Melting time (h)	Content (mol%)					O:P ratio
				P ₂ O ₅	Na ₂ O	SiO ₂	Al ₂ O ₃		
900Pt1 *	900	Platinum	1	58.24 ± 1.5	32.42 ± 0.9	9.34 ± 0.2	n.d.	2.9	
900Al1		Alumina	1	54.26 ± 1.9	33.81 ± 1.9	10.52 ± 0.6	1.42 ± 0.2	3.0	
900Al3			3	53.99 ± 1.9	33.72 ± 1.9	10.01 ± 0.6	2.24 ± 0.2	3.1	
900Al6			6	55.68 ± 1.9	32.62 ± 1.8	9.53 ± 0.5	2.15 ± 0.2	3.0	
900Al12		Fused silica	12	54.07 ± 1.9	32.89 ± 1.9	10.50 ± 0.6	2.52 ± 0.2	3.1	
1200Si0.5	1200		0.5	53.84 ± 1.9	33.55 ± 2.0	12.69 ± 0.7	n.d.	3.0	
1200Al1			1	53.89 ± 1.9	32.71 ± 1.8	9.76 ± 0.5	3.63 ± 0.3	3.1	
1200Al6		Alumina	6	50.85 ± 1.6	31.39 ± 1.8	8.85 ± 0.5	8.91 ± 0.4	3.2	
1200Al12			12	50.78 ± 1.6	30.74 ± 1.7	8.75 ± 0.5	9.74 ± 0.5	3.3	
Nominal composition			60	30	10	-	2.9		

Note: Actual composition of samples was analyzed by EDX or *ICP-OES.
Abbreviation: n.d., not detected.

2.4 | Structural investigation

MAS NMR spectroscopy provides important structural information on short to intermediate length scales. Standard single pulse acquisition (Bloch decay) ³¹P MAS NMR experiments were performed on a Bruker Avance III 300 MHz (7 T) spectrometer using a 4 mm MAS probe with a resonance frequency of 121.4 MHz. Typical delay times of 300-500 seconds and pulse lengths of 6 μs were used. Measurements were performed at MAS spinning frequencies of 10 kHz. Chemical shifts were referenced to concentrated (80%) H₃PO₄. ²⁷Al MAS NMR experiments were performed on a Varian VNMRs 500 (11 T) spectrometer using a Varian 1.6 mm T3 MAS probe with a resonance frequency of 130 MHz. Typical delay times of 1-2 seconds and pulse lengths of 0.5 μs were used. Measurements were performed at MAS spinning frequencies of 10 kHz. Chemical shifts were referenced to a 1 M aqueous solution of Al(NO₃)₃. ³¹P{²⁷Al}-REAPDOR NMR experiments were performed on a Bruker Avance III 300 MHz spectrometer, employing π-pulse lengths of 10.5 μs for ³¹P. The ²⁷Al dephasing pulse was set to 1/3 of the rotor period with an RF amplitude of 42 kHz. ²⁷Al{³¹P}-REDOR (rotational echo double resonance) NMR³⁵⁻³⁷ was performed on a Bruker Avance III 300 MHz using typical π-pulse lengths of 10 μs for ²⁷Al and 11 μs for ³¹P.

Raman spectra were recorded from 215 to 1500 cm⁻¹ (Renishaw RM2000 connected to a Leica microscope with 50× objective), using the 514 nm line of an Argon laser as excitation source. Selected samples were further investigated by Fourier-transform infrared spectroscopy (Vertex 80v, Bruker) under vacuum in the measurement range from 30 to 7500 cm⁻¹. Kramers-Kronig transformation was used for extracting the spectral absorption coefficient α(ν) in the range from 30 to 1800 cm⁻¹.

2.5 | Elastic properties

Elastic properties were characterized by ultrasonic echography on co-planar, optically polished glass discs with a thickness of about 1-2 mm. Values of longitudinal (c_L) and transversal (c_T) sound wave velocities were measured by ultrasonic echometry (Echometer 1077, Karl Deutsch GmbH & Co. KG), using piezoelectric transducers operating at frequencies of 8-12 MHz. From these results, longitudinal (L), shear (G), bulk (K), Young's modulus (E), as well as Poisson's ratio (ν) were calculated according to the following equations³⁸:

$$L = \rho c_L^2 \quad (1)$$

$$G = \rho c_T^2 \quad (2)$$

$$K = \rho \left(c_L^2 - \frac{4}{3} c_T^2 \right) \quad (3)$$

$$E = \rho \left[\frac{3c_L^2 - 4c_T^2}{(c_L/c_T)^2 - 1} \right] \quad (4)$$

$$v = \frac{c_L^2 - 2c_T^2}{2(c_L^2 - c_T^2)} \quad (5)$$

3 | RESULTS AND DISCUSSION

Chemical analysis (Table 2) confirmed that elements from the crucible material, aluminum^{25–30} or silicon,³⁹ were incorporated into the glasses during melting. Particularly at higher melting temperatures, that is, 1200°C compared to 900°C, significant alumina incorporation occurred, with maximum concentrations reaching 10 mol% Al₂O₃. In addition, analyzed phosphate contents were lower than the nominal ones, possibly owing to volatilization during melting. This would be expected to be more pronounced with increased melting temperatures and times, but no such trend was observed. On further consideration, a more important factor is the absolute dilution of the parent glass composition (P₂O₅, Na₂O, SiO₂) by crucible material (Al₂O₃ or SiO₂). It is not surprising that the best agreement with the nominal composition was found for the sample melted in a platinum crucible for 1 hour. The alumina crucible used for the preparation of glass 900Al6 was chosen for crucible analysis by EDX. It revealed that the selected part of the crucible wall, which was not in contact with the silicophosphate glass melt, consist of Al₂O₃ only.

However, even after melting, EDX analyses of the inner bottom part of the crucible demonstrated no evidence for diffusion of ions from the glass melt into the crucible wall. This indicates that crucible material was dissolved into the glass, as expected, rather than any ion exchange occurring between the two materials.

A slight increase in density (ρ) was observed for glass 900Al1 prepared in an alumina crucible at 900°C for 1 hour (2.51 g cm⁻³) compared to glass 900Pt1 prepared in a platinum crucible (2.49 g cm⁻³). An increase in melting time did not result in any marked changes in density for samples prepared at 900°C (Figure 1A), owing to low Al₂O₃ additions (1.42–2.52 mol%) and the relatively constant O:P ratio of about 3. Reference glass 1200Si0.5 prepared in a fused silica crucible at 1200°C had a density of 2.51 g cm⁻³. The density of glasses melted in alumina crucibles at 1200°C, by contrast, was strongly affected by the melting time and increased from 2.51 to 2.55 g cm⁻³ as the melting time increased from one to 12 hours (Figure 1B), owing to more pronounced incorporation of alumina (3.63–9.74 mol%). Glass density is influenced by the atomic weight of glass components and the glass structure (in turn affecting cross-linking). Because of the incorporation of Al₂O₃ from alumina or SiO₂ from fused silica crucibles into the melt, glasses prepared in either of these crucibles showed higher density values and lower molar volumes than the glass melted in a platinum crucible. Besides the glass density, thermal properties were also affected by leaching of crucible material

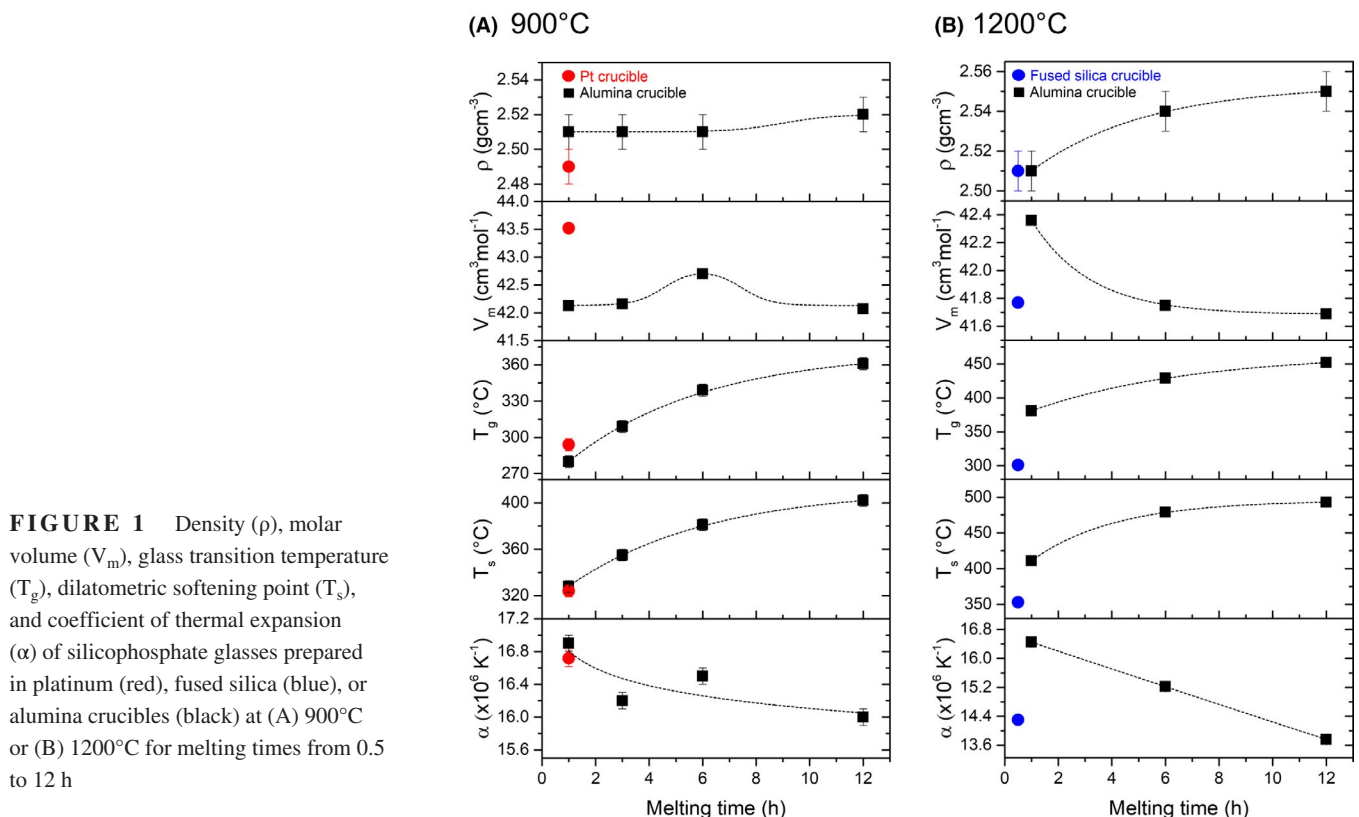


FIGURE 1 Density (ρ), molar volume (V_m), glass transition temperature (T_g), dilatometric softening point (T_s), and coefficient of thermal expansion (α) of silicophosphate glasses prepared in platinum (red), fused silica (blue), or alumina crucibles (black) at (A) 900°C or (B) 1200°C for melting times from 0.5 to 12 h

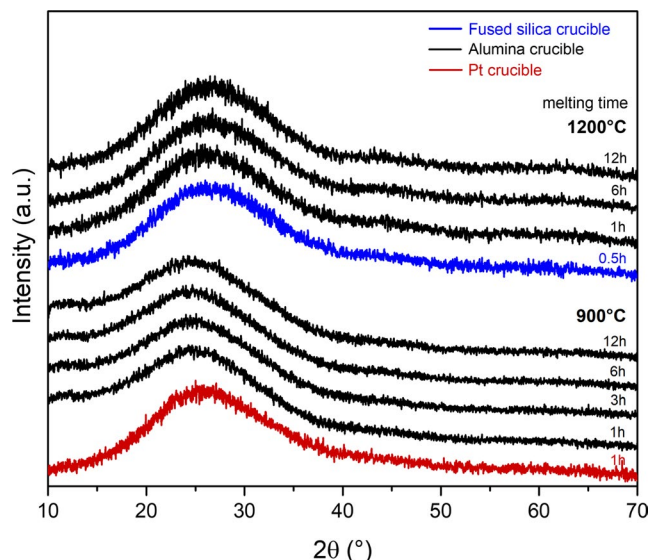


FIGURE 2 X-ray powder diffraction patterns of glasses prepared in platinum (red), fused silica (blue), or alumina crucibles (black) at 900°C or 1200°C for melting times from 0.5 to 12 h

into the melt as shown for glass-transition temperature (T_g), softening point (T_s), and coefficient of thermal expansion (α) in Figure 1 for glasses melted at 900°C (Figure 1A) or 1200°C (Figure 1B). Increasing melting times in alumina crucibles resulted in an increase in T_g and T_s , whereas α decreased. Al^{3+} , contrary to Na^+ , is a very effective cross-linker owing to its high field strength,^{29,30,40} which is reflected in higher bond energies, increasing T_g and lower α . The effect of alumina on thermal properties, again, was much more pronounced for glasses melted at higher temperatures owing to increased alumina incorporation.

X-ray diffraction patterns showed the typical amorphous halos with no traces of sharp diffraction peaks, confirming that the glasses were obtained without crystallization occurring (Figure 2). A shift in the maxima of the amorphous halos of XRD patterns with increasing melting time in alumina crucibles already hinted at structural changes occurring, and this was confirmed by vibrational (Figures 3 and 4) and solid-state NMR spectroscopy (Figures 5 and 6).

Figure 3A presents Raman spectra of glasses melted in platinum and alumina crucibles at 900°C with varying melting times. Starting with the spectrum of aluminum-free glass 900Pt1, we note that the high-frequency Raman components at about 1349 and 1298 cm^{-1} can be associated with Q^3 and Q^2 phosphate units, respectively. Q^n indicates a phosphate tetrahedral unit with n bridging oxygen atoms connecting to a neighboring PO_4 tetrahedron. The band at 1349 cm^{-1} can be attributed to the stretching mode of the $\text{P}=\text{O}$ double bond, $\nu(\text{P}=\text{O})$, of the Q^3 unit and the band at about 1298 cm^{-1} to the asymmetric stretching mode of the PO_2^- group in Q^2 units, $\nu_{\text{as}}(\text{PO}_2^-)$, in metaphosphate chains or rings.^{29,30,39,41–45} The Raman bands at 1156 and

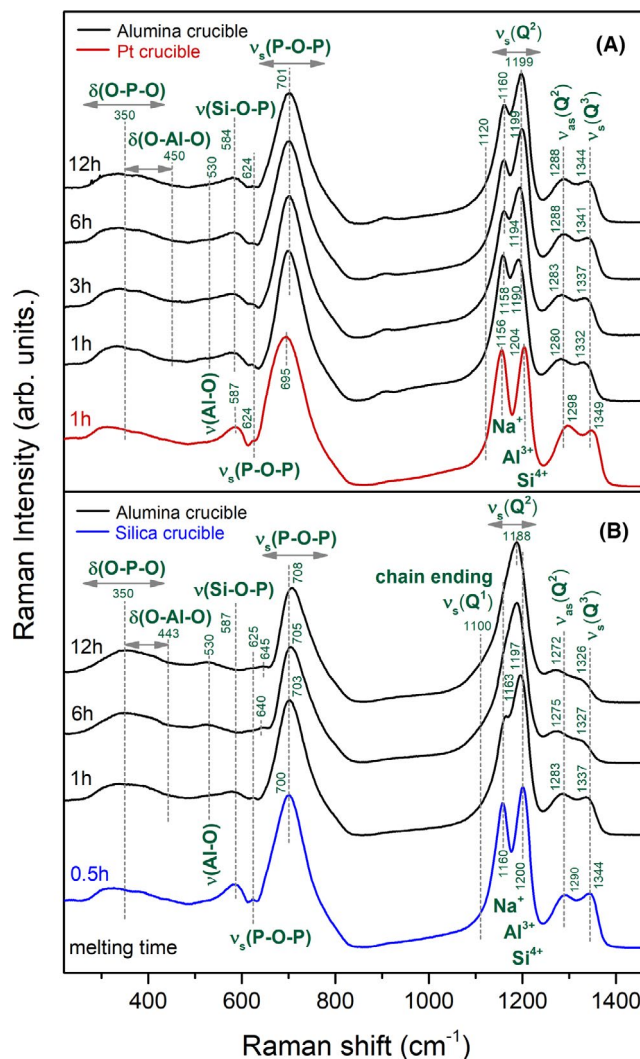


FIGURE 3 Raman spectra of silicophosphate glasses prepared in platinum (red), fused silica (blue) or alumina crucibles (black) at (A) 900°C or (B) 1200°C for melting times from 0.5 to 12 h

1200 cm^{-1} are characteristic for the symmetric stretching mode of Q^2 units, $\nu_s(\text{PO}_2^-)$. The lower energy band is typical for symmetric P–O stretching modes of Q^2 units charge-balanced by Na^+ ,^{43,46} whereas the separate band at 1204 cm^{-1} arises from the symmetric stretching modes of the Q^2 units charge-balanced by higher charged cations such as Si^{4+} (but also Al^{3+} , as discussed later).^{43,46,47} The strong broad band at 695 cm^{-1} is caused by the symmetric stretching of P–O–P bridges, $\nu_s(\text{P–O–P})$, connecting Q^2 units, whereas the very weak band at 624 cm^{-1} can be attributed to the $\nu_s(\text{P–O–P})$ mode of P–O–P bridges connecting Q^3 units in a three-dimensional phosphate network. The presence of P–O–Si bonds in glass 900Pt1 is signaled by the band at 587 cm^{-1} , which can be associated to the symmetric stretching of P–O–Si bonds, $\nu_s(\text{P–O–Si})$.⁴⁸

Melting in alumina crucibles, particularly when increasing the melting temperature and time, caused major modifications to the silicophosphate glass structure as

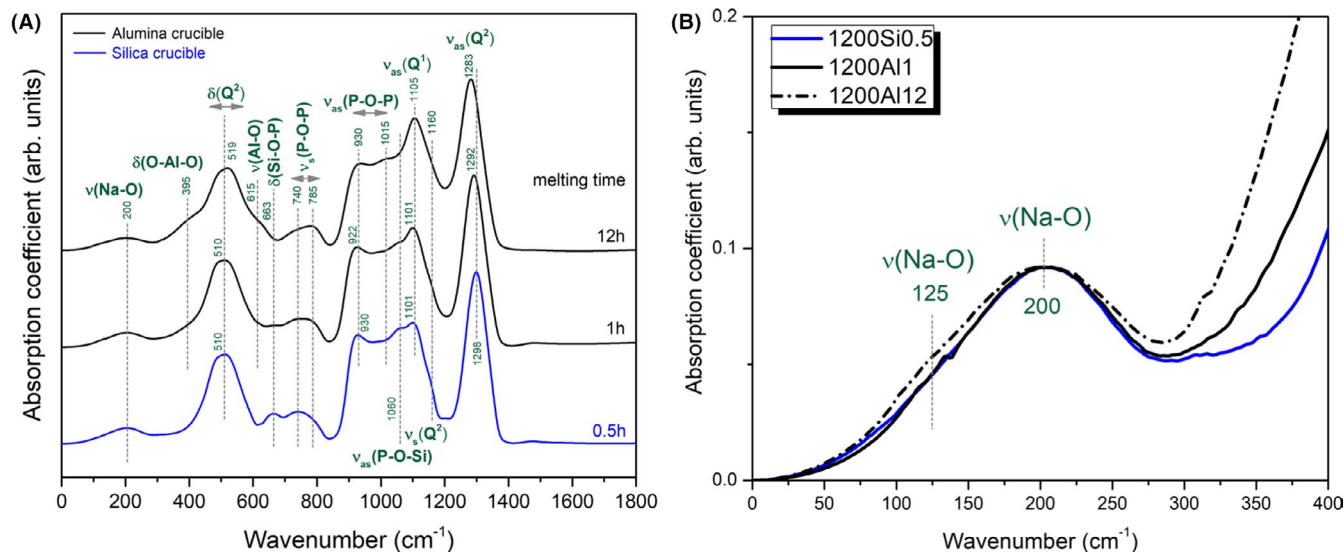
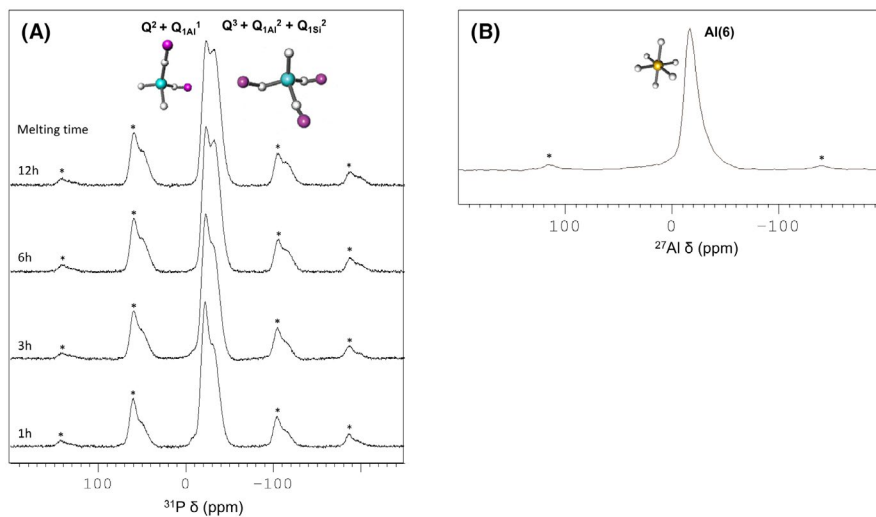


FIGURE 4 A, IR spectra of silicophosphate glass melted at 1200°C in a fused silica crucible (blue) for 0.5 h and alumina crucibles (black) for 1 or 12 h. B, Far-IR spectra of silicophosphate glasses melted at 1200°C in a fused silica crucible (blue) for 0.5 h and alumina crucibles (black) for 1 or 12 h showing changes in band width and a Na^+ ion motion band at about 200 cm^{-1} . Far-infrared spectra were scaled to have the same intensity at 200 cm^{-1}

FIGURE 5 A, ^{31}P MAS NMR spectra of silicophosphate glasses melted in alumina crucibles at 900°C between 1 and 12 h. The low-intensity signal at -12.5 ppm in the glass melted for 1 h can be traced back to minor amounts of Q^1 units. B, A typical ^{27}Al MAS NMR spectrum of silicophosphate glass 900A11, melted in an alumina crucible at 900°C for 1 hour, showing aluminum present in sixfold coordination (asterisks indicate spinning sidebands)



reflected in the Raman spectra shown in Figure 3. Glasses melted in alumina crucibles exhibited progressive changes with melting time in the relative intensity and position of characteristic Raman bands compared to the glass melted in a platinum crucible (900Pt1). A band evolving at 1188 to 1199 cm^{-1} suggests the formation of P–O–Al bridges, since it can be attributed to $\nu_{\text{s}}(\text{PO}_2^-)$ modes of Q^2 units cross-linked by P–O–Al bonds, that is, charge-balanced by Al^{3+} (and Si^{4+}) rather than Na^+ .^{29,42,43,49} The symmetric stretching modes of Q^2 connected to Al^{3+} , that is, P–O–Al bonds, found at 1188 cm^{-1} in Figure 3B are broader than the other symmetric stretching modes of P–O in Q^2 units at 1156 and 1204 cm^{-1} , as coupling of Al–O–P bonds occurs.⁴³ Following the charges of the modifier cations $\text{Na}^+ < \text{Al}^{3+} < \text{Si}^{4+}$, the frequency of the P–O symmetric

stretching mode of Q^2 units shifts to higher energies as the valence of the bonded cation increases, that is from Na^+ (1165 cm^{-1}) to Al^{3+} (1188 cm^{-1}) or to Si^{4+} (1204 cm^{-1}). As Al_2O_3 dissolved into the glass, the O:P ratio increased from 2.9 (900Pt1) to 3.1 (900A112). This might be reflected in an intensity increase in the low-energy shoulder near 1120 cm^{-1} from glass 900Pt1 (Q^2 units in longer chains) to 900A112, with more Q^2 units next to chain-terminating Q^1 .^{29,42,43} The symmetric stretching modes of these chain-terminating Q^1 units would be found near 1050 cm^{-1} but are only apparent as weak shoulder or tail broadening in the Raman spectra of the 900°C series shown in Figure 3A. The strongest Raman band at 695 cm^{-1} , mentioned above, shifted to 701 cm^{-1} with Al_2O_3 incorporation. The weak Raman bands below 650 cm^{-1} are harder to assign to

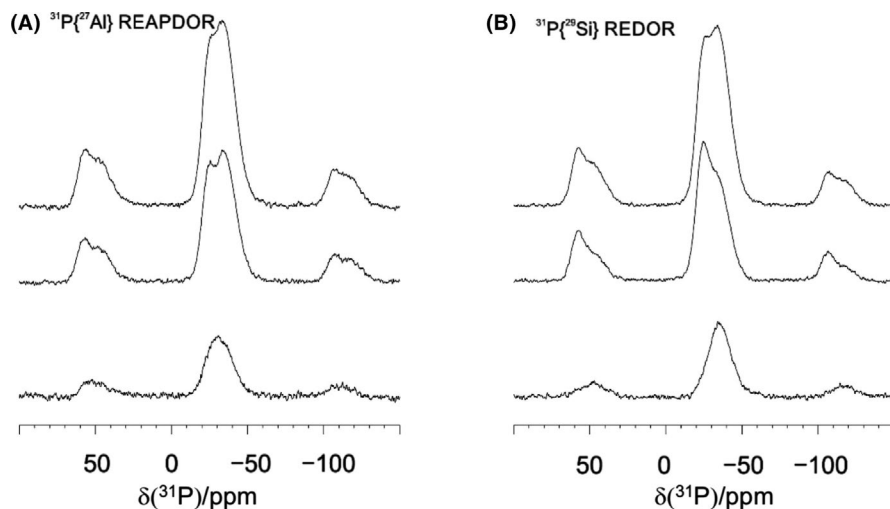


FIGURE 6 A, $^{31}\text{P}\{^{27}\text{Al}\}$ REAPDOR and B, $^{31}\text{P}\{^{29}\text{Si}\}$ REDOR NMR spectra, obtained at 32 rotor cycles and a MAS frequency of 10 kHz. Top spectra represent rotor synchronized ^{31}P spin echo spectra; middle spectra the actual REAPDOR (A) or REDOR (B) spectra with the dephasing pulse(s) on ^{27}Al (A) or ^{29}Si (B); bottom spectra: difference of the two above

specific vibrational modes, as bending of Y–O–Y' and of O–Y–O, with Y, Y' = P, Al, Si in all possible variations, are likely to contribute, as well as general network deformation modes. Only the 587 cm^{-1} P–O–Si band of the 900Pt1 glass (melted in platinum crucible) is assigned readily; it shifted to 584 cm^{-1} with Al^{3+} incorporation and lost relative intensity, indicating the reduction in the relative population of P–O–Si bonds. This low-intensity broad vibrational band of $\nu(\text{Si–O–P})$ at 584 cm^{-1} seemed unaffected by increasing melting times, appearing at the same frequencies for all glasses prepared in alumina crucibles, as was the weak contribution at 624 cm^{-1} and the band at 920 cm^{-1} . The introduction of Al^{3+} ions in the glass, leached from the alumina crucible, was further supported by the appearance of the weak band at about 530 cm^{-1} , caused by Al–O stretching, $\nu(\text{Al–O})$,⁵⁰ and the shoulder at 350 to 450 cm^{-1} caused by O–Al–O bending, $\delta(\text{O–Al–O})$.^{42,43} The last two features were observed only in the Raman spectra of glasses synthesized in alumina crucibles.

Structural changes owing to Al_2O_3 incorporation appeared even more pronounced for higher melting temperatures (1200°C compared to 900°C ; Figure 3B). As the melting time increased from 1 to 12 hours at 1200°C , the band at about 1160 cm^{-1} (corresponding to Q^2 units charge-balanced by Na^+) gradually decreased in relative intensity and merged with the broad band developing at about 1188 cm^{-1} , the latter feature corresponding to Q^2 units charge-balanced by higher-charged cations, here Al^{3+} , and confirmed the cross-linking of Q^2 units by P–O–Al–O–P bonds. With increasing melting time the stretching vibration (ν_s) of the P–O–P band near 700 cm^{-1} was found to shift to 708 cm^{-1} with melting time, whereas the asymmetric stretching vibration of Q^2 units shifted from 1290 to 1272 cm^{-1} , and the symmetric stretching vibration of Q^3 units shifted from 1344 to 1326 cm^{-1} . These down-shifts are consistent with an increased degree of depolymerization

as the O:P ratio increased from 2.9 to 3.3 (cf. Table 1). Accordingly, a distinct shoulder developed near 1100 cm^{-1} with increasing melting time in alumina crucibles, which can be attributed to the symmetric P–O stretching mode of Q^1 units.^{43,46,51} For the longest melting times the distinct $\nu_s(\text{P–O–Si})$ band (present at 587 cm^{-1} for the glasses melted in platinum or silica crucibles) disappeared completely, owing to the dominant formation of P–O–Al bonds (Figure 3B). Comparing the effect of temperature, we note that the Raman spectrum of glass 900Al12, alumina-melted glass at 900°C for 12 hours, still shows the $\nu_s(\text{PO}_2^-)$ band at 1161 cm^{-1} , which is characteristic for Q^2 in metaphosphate chains, as seen in Figure 3A. By contrast, glass 1200Al12, melted for the same duration at 1200°C , only showed a very weak shoulder here.

The spectrum of glass 1200Si0.5 (Figure 3B), prepared in a fused silica crucible at 1200°C , shows that the $\nu_s(\text{P–O–Si})$ band⁴⁸ at about 587 cm^{-1} has gained relative intensity in comparison to the same band of the 900Pt1 spectrum in Figure 3A. This indicated an increased number of P–O–Si bridging bonds upon melting in silica crucible, owing to incorporation of additional silica from the crucible. In addition, the $\nu(\text{PO}_2^-)$ band of Q^2 units charge-balanced by Na^+ at about 1160 cm^{-1} has lost intensity relative to the same mode of Q^2 sites charge-balanced by Si^{4+} at 1200 cm^{-1} .

Three selected silicophosphate compositions (melted in silica or alumina crucibles at 1200°C for 0.5, 1200Si0.5, 1, 1200Al1, or 12 hours, 1200Al12) were additionally analyzed by infrared reflectance spectroscopy. The calculated absorption coefficient spectra are depicted in Figure 4 and further demonstrate the structural effect of crucible material incorporation on the glass structure.

The presence of P–O–Si bonds was inferred by the bands observed at about 1060 and 663 cm^{-1} in the spectrum of glass 1200Si0.5, as they can be attributed to $\nu_{\text{as}}(\text{P–O–Si})$ and $\delta(\text{P–O–Si})$ modes, respectively.^{48,49,52,53} This sample,

TABLE 3 ^{31}P MAS NMR and ^{27}Al MAS NMR results of silicophosphate glasses prepared in alumina crucibles at 900°C for melting times from 1 to 12 h

Sample	Melting time (h)	^{31}P MAS NMR					
		Q^1		$\text{Q}^2 + \text{Q}_{\text{Al}}^1$		$\text{Q}^3 + \text{Q}_{\text{Al}}^2 + \text{Q}_{\text{Si}}^2$	
		Area (%)	Chem. shift (ppm)	Area (%)	Chem. shift (ppm)	Area (%)	Chem. shift (ppm)
900Al1	1	5	−13.6	36	−21.6	58	−31.8
900Al3	3	3	−12.8	30	−21.8	66	−32.0
900Al6	6	2	−15.8	28	−22.1	70	−32.5
900Al12	12	—	—	28	−21.9	71	−32.6

prepared in fused silica crucible, is free of Al^{3+} ions and such bands were not observed in Si-free metaphosphate glasses.^{40,43}

Both of these Si-related bands lose relative intensity or merge with neighboring bands during prolonged melting in alumina crucibles, whereas new bands appear at about 615 cm^{-1} , $\nu(\text{Al}-\text{O})$,⁵⁰ and 395 cm^{-1} , $\delta(\text{O}-\text{Al}-\text{O})$,^{42,43} as a result of the incorporation of Al^{3+} ions from the alumina crucible. These latter bands are particularly intense in the infrared spectrum of glass 1200Al12.

The development of IR spectra with Al_2O_3 and SiO_2 incorporation is in good agreement with the Raman spectra (Figure 3), although more bands are IR active and, thus, more vibrational modes overlap. The high-frequency range is dominated by a strong band peaking in the range from 1283 to 1298 cm^{-1} , owing to the $\nu_{\text{as}}(\text{PO}_2^-)$ mode of the PO_2^- group in Q^2 units.^{29,30,39,42–45} This band of Q^2 units at about 1300 cm^{-1} exhibits some contribution from Q^3 units on the high-energy side, and the down-shift of this band from 1298 to 1283 cm^{-1} reflects the higher degree of depolymerization, as the number of Q^3 units decreased and more Q^1 units formed for longer melting times at 1200°C in Al_2O_3 crucibles.^{42,43} We note that increasing melting times in alumina crucibles up to 12 hours caused a reduction in the relative intensity of the $\nu_{\text{as}}(\text{PO}_2^-)$ band, which is consistent with the shortening of metaphosphate chains²⁹ and their cross-linking by P–O–Al bridges as revealed by Raman spectroscopy. In agreement with Raman spectroscopy results, IR spectra here give clear indication for the depolymerization of the phosphate network, indicated by the change in the O:P ratio of the analyzed compositions, which increased from 2.9 to 3.3. Additional evidence for the shortening of metaphosphate chains is provided from the IR band developing at about 1105 cm^{-1} , which was assigned to the $\nu_{\text{as}}(\text{PO}_3^{2-})$ mode of PO_3^{2-} (Q^1) units forming the ends of shorter chains.²⁹ This band is only apparent as one of several features of a broader band envelope for samples melted for 1 hour at 1200°C , 1200Al1, but develops into a strong band at 12 hours' melting, 1200Al12. The low-energy side can actually be deconvoluted into several bands of P–O–P bonds in chains or in larger and smaller rings.^{42,43} An up-shift

of the asymmetric stretching P–O–P mode from about 922 to 930 cm^{-1} can be attributed to a larger number of shorter metaphosphate chains and the change in the charge-balancing modifier cations from Na^+ to Al^{3+} or Si^{4+} .⁴³

In the far-infrared parts of the spectra (Figure 4B), the band at about 200 cm^{-1} can be assigned to vibrations of Na^+ ions, $\nu(\text{Na}-\text{O})$, within their oxygen coordination polyhedra as found in previous studies on sodium phosphate^{42,43} and sodium silicate^{54,55} glasses. While the central frequency of this band remains almost unaffected by melting time and crucible material, a broadening towards lower frequencies (125 cm^{-1}) was observed for melting in alumina crucible for 12 hours. This indicates a broadening in the distribution of oxide sites available to Na^+ ions, and it agrees with earlier findings in sodium aluminosilicate glasses.^{55,56}

Figure 5 illustrates ^{31}P MAS NMR and ^{27}Al MAS NMR spectra of glasses prepared in alumina crucibles at 900°C with melting times increasing from 1 to 12 hours. The ^{27}Al MAS NMR spectra of all glasses (shown in Figure 5B for sample 900Al1 prepared at 900°C for 1 hour) present a single resonance at -10.5 ppm , which was assigned to six-coordinated aluminum.⁵⁷ The ^{27}Al MAS NMR profile did not change with melting time, confirming exclusive sixfold coordination for aluminum in all aluminum-containing glasses in this study. The introduction of Al^{3+} and O^{2-} from alumina crucibles resulted in a gradual change in the silicophosphate glass network. ^{31}P MAS NMR spectra are mostly composed of two peaks, which are in the range typically assigned to Q^3 (about -32 ppm) and Q^2 units (about -21 ppm). The results of deconvolution of the ^{31}P MAS NMR spectra, performed with the software DMFIT⁵⁸ are collected in Table 3. All spinning sidebands were included to obtain the area of the three identified signals.

However, it is not possible to identify contributions to ^{31}P signals from P–O–Si or P–O–Al bonds based on the chemical shift alone. MAS NMR cannot distinguish between Q^n groups, that is, phosphate tetrahedra connected to n neighboring phosphate tetrahedra, and $\text{Q}_{\text{Al}}^{n-1}$ or $\text{Q}_{\text{Si}}^{n-1}$ groups, that is, phosphate tetrahedra connected to $n-1$ phosphate tetrahedra and one aluminum or one silicon atom, respectively.⁵⁹

P–O–Si bonds detected by vibrational spectroscopy for the aluminum-free glasses, 900Pt1 and 1200Si0.5, are therefore likely to be included in these two signals as Q_{Si}^2 groups. These structural motifs can, however, be safely identified exploring the magnetic dipole couplings between ^{31}P and ^{29}Si or between ^{31}P and ^{27}Al employing dipolar-based NMR methods such as $^{31}\text{P}\{^{27}\text{Al}\}$ -REAPDOR and $^{31}\text{P}\{^{29}\text{Si}\}$ -REDOR NMR spectroscopy. Owing to the limited Si content of the samples and the low natural abundance of the NMR-active ^{29}Si isotope, these measurements were conducted using a sample of the composition 0.97 (0.3 Na_2O -0.6 P_2O_5 -0.1 SiO_2)-0.03 Al_2O_3 , which was 100% enriched in ^{29}Si and contained small amounts of MnO to shorten the T_1 -relaxation times.

$^{31}\text{P}\{^{27}\text{Al}\}$ REAPDOR and $^{31}\text{P}\{^{29}\text{Si}\}$ REDOR NMR spectra, obtained for 32 rotor cycles and a MAS frequency of 10 kHz, are shown in Figure 6. In both cases, the existence of the difference signal indicates spatial proximity between P and Al and P and Si, respectively. The positions of the difference signals are -29 ppm for the $^{31}\text{P}\{^{27}\text{Al}\}$ -REAPDOR and -35 ppm for the $^{31}\text{P}\{^{29}\text{Si}\}$ -REDOR NMR experiment. These are typical values for Q_{Al}^2 and Q_{Si}^2 units, thus confirming that the upfield signal at -32 ppm contains contributions from Q_{Al}^2 and Q_{Si}^2 and corroborating results from Raman and IR spectroscopy.

This also explains the increase in intensity of the -32 ppm signal with increasing melting time. We assigned this to an increasing amount of Q_{Al}^2 units contributing to the signal. This signal is shifting downfield at higher concentrations of incorporated Al, leading to a merging of the signals into a single, non-resolved ^{31}P signal at higher Al content, as observed in our previous study.³¹ This means that with increasing aluminum content in the glass, the relative amount of Q_{Al}^2 groups increased, while the amount of Q^2 groups not connected to Al decreased (Figure 5A).

Further information about dominating connectivity motifs could be obtained from a variety of additional dipolar NMR experiments including $^{27}\text{Al}\{^{31}\text{P}\}$ REDOR NMR, $^{29}\text{Si}\{^{31}\text{P}\}$ REDOR NMR, and $^{29}\text{Si}\{^{27}\text{Al}\}$ REDOR NMR. $^{27}\text{Al}\{^{31}\text{P}\}$ REDOR data on the enriched glass sample³¹ and the sample melted for 12 hours (900Al12; Figure 7) clearly revealed Al to be fully coordinated by phosphorous, that is, to be present in $\text{Al}(\text{OP})_6$ units. While Si exclusively adopted sixfold coordination in the Al-free base glass, a fraction of Si was being converted to Si in fourfold coordination upon incorporation of Al (see Figure S1 and our previous study³¹). From $^{29}\text{Si}\{^{31}\text{P}\}$ REDOR NMR on the enriched sample (see Figure S1) it was found that hexa-coordinate Si was virtually fully coordinated by six phosphate units, in agreement with our recent findings.¹⁰ For tetrahedral Si, the analysis was hampered by considerable noise owing to the low percentage of SiO_4 groups in the samples. However, the result was compatible with 3–4 P neighbors per SiO_4 tetrahedron, which is also in line with the observed chemical shift of -120 ppm.¹²

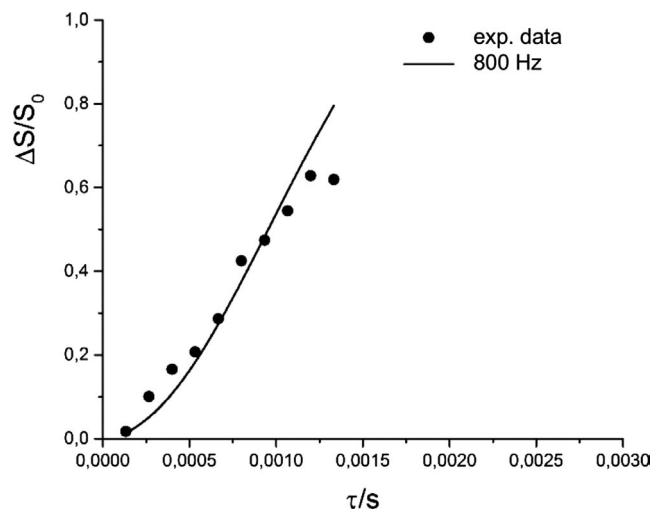


FIGURE 7 $^{27}\text{Al}\{^{31}\text{P}\}$ -REDOR NMR data (black filled circles) for glass sample 900Al12 together with the results of a SIMPSON simulation assuming an effective dipolar coupling of 800 Hz, which translates into individual Al–P distances of 3.2 Å

Correspondingly $^{29}\text{Si}\{^{27}\text{Al}\}$ REAPDOR NMR experiments (data not shown) only gave a negligible effect.

Combining our findings with the results from our previous study,³¹ we propose that network rigidity and stability of the glass are increased as sixfold-coordinated aluminum from corrosion of the alumina crucible adds its high cross-linking strength to sixfold-coordinated silicon. At longer melting times, the amount of Al^{3+} ions diffused into the glass and, subsequently, the number of Q_{Al}^1 and Q_{Al}^2 increased, leading to strengthening of the phosphate structure with P–O–Al–O–P cross-links. Al^{3+} was fully connected to phosphate species, replacing silicon atoms.

These structural changes were also reflected in the elastic properties of the glasses, including longitudinal (L), shear (G), bulk (K), and Young's moduli (E) as well as Poisson's ratio (ν) (Figure 8). In agreement with the relatively constant density (Figure 1A) mentioned above, only minor changes in the elastic properties were noticed for glasses melted in alumina crucibles at 900°C (Figure 8A). Increasing the melting time from 1 to 12 hours resulted in a marginal increase in G from (17.6 ± 0.2) to (17.9 ± 0.2) GPa, whereas E remained constant within the error limits, that is, (44.9 ± 1.1) GPa as compared to (45.3 ± 1.1) GPa. Contrary to this, L and K decreased slightly from (57.4 ± 0.7) to (56.2 ± 0.5) GPa and from (34.0 ± 0.8) to (32.3 ± 0.8) GPa, respectively, with increasing melting time from 1 to 12 hours. Likewise, ν was reduced from 0.280 ± 0.008 to 0.267 ± 0.008 . By comparison, more pronounced changes in L, G, K, and E are discernible for glasses prepared in alumina crucibles at 1200°C (Figure 8B). The values of L, G, K, and E first increased with melting time from 1 to 6 hours and then dropped slightly at 12 hours. Interestingly, ν showed the opposite

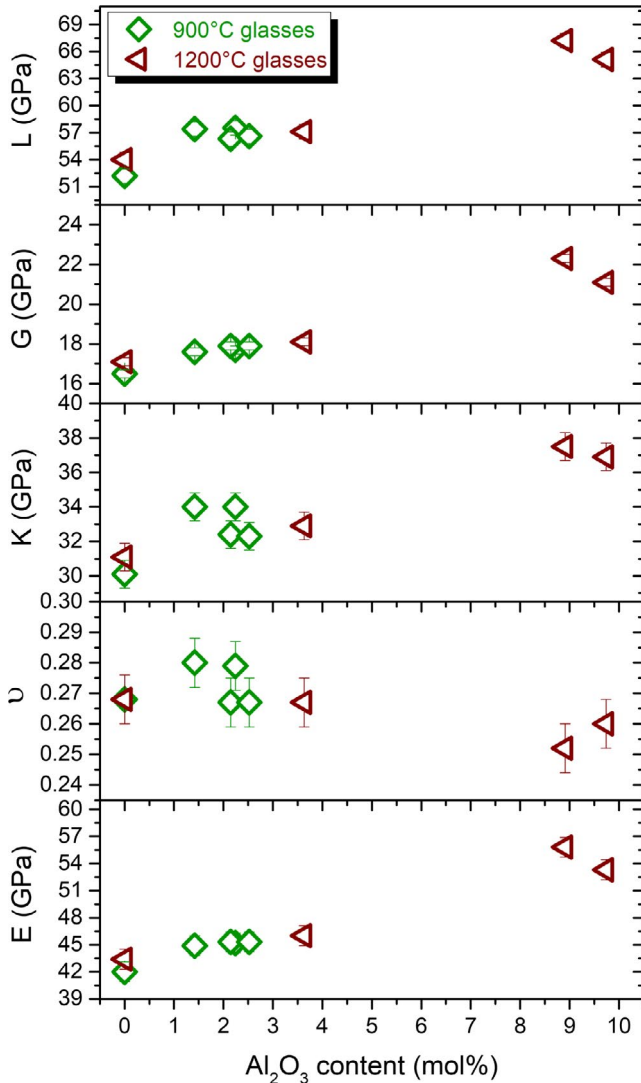


FIGURE 8 Compositional dependence of the elastic properties of silicophosphate glasses prepared at 900°C (green) and 1200°C (red) on the Al₂O₃ content: Longitudinal modulus (L), shear modulus (G), bulk modulus (K), Poisson's ratio (ν), and Young's modulus (E)

trend, decreasing from 0.267 ± 0.008 to 0.252 ± 0.008 with increasing melting time from 1 to 6 hours, followed by a minor increase to 0.260 ± 0.008 at 12 hours. The latter findings in combination with the results from the glasses melted in alumina crucibles at 900°C indicate an overall increase in L, G, K, and E along with a slight reduction of ν with increasing melting time and temperature and, thus, higher Al₂O₃ concentration. These trends are in good agreement with previous observations,^{51,60} and support the conclusions derived from our thermal (Figure 1) and structural analyses (Figures 3–5) that the introduction of Al₂O₃ from alumina crucibles strengthens the glass network through the creation of P–O–Al–O–P cross-links between the phosphate chains, thus enhancing overall network rigidity and connectivity.⁶¹ Moreover, the compositional tendency of ν agrees well with a commonly accepted model according to

which glasses with a higher network dimensionality typically exhibit smaller values of ν as compared to glasses with a weakly cross-linked network structure.⁶²

4 | CONCLUSIONS

Al₂O₃ and SiO₂ leaching from alumina and fused silica crucibles, respectively, into a silicophosphate melt caused depolymerization of the phosphate network, replacing P–O–P bonds by either P–O–Al or P–O–Si bonds. Silicon, which was present in sixfold coordination exclusively in the starting glass, was replaced by aluminum, creating some fourfold-coordinated silicon. Aluminum was present in sixfold coordination exclusively. These structural changes significantly affected glass density, thermal properties as well as elastic properties. Alumina incorporation was significantly increased with melting temperature, whereas the effect of melting time was less pronounced. Therefore, if alumina incorporation is undesired, glass preparation at lower temperature is an effective means of reducing alumina leaching. Taken together, the findings of this study emphasize the pronounced effects of alumina incorporation on the structure and, subsequently, on the properties of silicophosphate glasses and highlight the need for quantitative analysis of the actual glass composition when using ceramic crucibles.

ACKNOWLEDGMENTS

The authors thank Dr Christian Bocker for SEM-EDX measurements. Financial support by DFG project BR 4608/5 (SPP 1594) is gratefully acknowledged. NS acknowledges funding by a Royal Thai Government scholarship under the Ministry of Science and Technology (MOST).

ORCID

Doris Möncke <https://orcid.org/0000-0002-4197-5520>

Lothar Wondraczek <https://orcid.org/0000-0002-0747-3076>

[org/0000-0002-0747-3076](https://orcid.org/0000-0002-0747-3076)

Efstathios I. Kamitsos <https://orcid.org/0000-0003-4667-2374>

[org/0000-0003-4667-2374](https://orcid.org/0000-0003-4667-2374)

Delia S. Brauer <https://orcid.org/0000-0001-5062-0695>

REFERENCES

1. Dupree R, Holland D, Mortuza MG. 6-coordinated silicon in glasses. *Nature*. 1987;328(6129):416–7.
2. Dupree R, Holland D, Mortuza MG, Collins JA, Lockyer M. An MAS NMR study of network-cation coordination in phosphosilicate glasses. *J Non-Cryst Solids*. 1988;106(1–3):403–7.
3. Dupree R, Holland D, Mortuza MG, Collins JA, Lockyer M. Magic angle spinning NMR of alkali phospho-alumino-silicate glasses. *J Non-Cryst Solids*. 1989;112(1–3):111–9.

4. Prabakar S, Rao KJ, Rao C. A MAS NMR investigation of lead phosphosilicate glasses - The nature of the highly deshielded 6-coordinated silicon. *Mater Res Bull.* 1991;26(4):285–94.
5. Miyabe D, Takahashi M, Tokuda Y, Yoko T, Uchino T. Structure and formation mechanism of six-fold coordinated silicon in phosphosilicate glasses. *Physical Review B.* 2005;71(17):172202.
6. Yamashita H, Yoshino H, Nagata K, Yamaguchi I, Ookawa M, Maekawa T. NMR and Raman studies of $\text{Na}_2\text{O-P}_2\text{O}_5\text{-SiO}_2$ glasses - Six-coordinated Si and basicity. *J Ceram Soc Jpn.* 1998;106(6):539–44.
7. Mudrakovskii IL, Mastikhin VM, Shmachkova VP, Kotsarenko NS. High-resolution solid-state ^{29}Si and ^{31}P NMR of silicon-phosphorus compounds containing six-coordinated silicon. *Chem Phys Lett.* 1985;120(4–5):424–6.
8. Handa K, Ide J, Yamamoto K, Kurosawa N, Ozutsumi K, Harami T, et al. Local structure of six-coordinated silicon in $\text{Li}_2\text{O-SiO}_2\text{-P}_2\text{O}_5$ glasses by transmission XAFS experiments. *Phys Scr.* 2005;T115:314–5.
9. Muthupari S, Fleet ME. XANES of sixfold silicon in $\text{MoO}_3\text{-SiO}_2\text{-P}_2\text{O}_5$ glasses. *J Non-Cryst Solids.* 1998;238(3):259–65.
10. Venkatachalam S, Schröder C, Wegner S, van Wüllen L. The structure of a borosilicate and phosphosilicate glasses and its evolution at temperatures above the glass transition temperature: lessons from in situ MAS NMR. *Eur J Glass Sci Tech B Phys Chem Glasses.* 2014;55(6):280–7.
11. Hermansen C, Guo XJ, Youngman RE, Mauro JC, Smedskjaer MM, Yue YZ. Structure-topology-property correlations of sodium phosphosilicate glasses. *J Chem Phys.* 2015;143(6):064510.
12. Weeding TL, Dejong B, Veeman WS, Aitken BG. Silicon coordination changes from 4-fold to 6-fold on devitrification of silicon phosphate glass. *Nature.* 1985;318(6044):352–3.
13. Canning J, Sceats MG, Inglis HG, Hill P. Transient and permanent gratings in phosphosilicate optical fibers produced by the flash condensation technique. *Opt Lett.* 1995;20(21):2189–91.
14. Zeng H, Jiang QI, Liu Z, Li X, Ren J, Chen G, et al. Unique sodium phosphosilicate glasses designed through extended topological constraint theory. *J Phys Chem B.* 2014;118(19):5177–83.
15. Lim J-M, Won J-H, Lee H-J, Hong YT, Lee M-S, Ko CH, et al. Polyimide nonwoven fabric-reinforced, flexible phosphosilicate glass composite membranes for high-temperature/low-humidity proton exchange membrane fuel cells. *J Mater Chem.* 2012;22(35):18550–7.
16. Brow RK, Kirkpatrick RJ, Turner GL. Local structure of $x\text{Al}_2\text{O}_3\text{-(1-x)NaPO}_3$ glasses: An NMR and XPS study. *J Am Ceram Soc.* 1990;73(8):2293–300.
17. Kishioka A, Hayashi M, Kinoshita M. Glass formation and crystallization in ternary phosphate systems containing Al_2O_3 . *Bull Chem Soc Jpn.* 1976;49(11):3032–6.
18. Neuville DR, Cormier L, Massiot D. Al coordination and speciation in calcium aluminosilicate glasses: Effects of composition determined by ^{27}Al MQ-MAS NMR and Raman spectroscopy. *Chem Geol.* 2006;229(1–3):173–85.
19. Kreidl NJ, Weyl WA. Phosphates in ceramic ware: IV, phosphate glasses. *J Am Ceram Soc.* 1941;24(11):372–8.
20. Brow RK. Nature of alumina in phosphate glass: I, properties of sodium aluminophosphate glass. *J Am Ceram Soc.* 1993;76(4):913–8.
21. Brow RK, Kirkpatrick RJ, Turner GL. Nature of alumina in phosphate glass: II, Structure of sodium aluminophosphate glass. *J Am Ceram Soc.* 1993;76(4):919–28.
22. Kreidl NJ. Recent studies on the fluorescence of glass. *J Opt Soc Am.* 1945;35(4):249–57.
23. Tooley F. The handbook of glass manufacture: A book of reference for the plant executive, technologist, and engineer: Books for the Glass Industry Division. New York, NY: Ashlee Publishing Company; 1984.
24. Tapasa K, Jitwatcharakomol T. Thermodynamic calculation of exploited heat used in glass melting furnace. *Procedia Engineering.* 2012;32(Supplement C):969–75.
25. Barz A, Haase T, Meyer K, Stachel D. Corrosion of crucible materials and their influence on structure of phosphate glasses. *Phosphorus Research Bulletin.* 1996;6:331–5.
26. Smith CE, Brow RK, Montagne L, Revel B. The structure and properties of zinc aluminophosphate glasses. *J Non-Cryst Solids.* 2014;386:105–14.
27. Parsons AJ, Burling LD, Rudd CD, Scotchford CA, Walker GS. The effect of production regime and crucible materials on the thermal properties of sodium phosphate glasses produced from salts. *J Biomed Mater Res B.* 2004;71B(1):22–9.
28. Bae BS, Weinberg MC. Oxidation-reduction equilibrium in copper phosphate-glass melted in air. *J Am Ceram Soc.* 1991;74(12):3039–45.
29. Palles D, Konidakis I, Varsamis C, Kamitsos EI. Vibrational spectroscopic and bond valence study of structure and bonding in Al_2O_3 -containing AgI-AgPO_3 glasses. *RSC Adv.* 2016;6(20):16697–710.
30. Konidakis I, Varsamis C, Kamitsos EI. Effect of synthesis method on the structure and properties of AgPO_3 -based glasses. *J Non-Cryst Solids.* 2011;357(14):2684–9.
31. Nizamutdinova A, Kirchain H, van Wüllen L, Sawangboon N, Brauer DS. The structural role of alumina in alkaliphosphosilicate glasses: A multinuclear solid state NMR. *Phys Chem Glasses: Eur J Glass Sci Technol B.* 2018;59(6):267–76.
32. Fischer B. Reduction of platinum corrosion in molten glass. *Platin Met Rev.* 1992;36(1):14–25.
33. Gullion T, Vega AJ. Measuring heteronuclear dipolar couplings for $I=1/2$, $S > 1/2$ spin pairs by REDOR and REAPDOR NMR. *Prog Nucl Magn Reson Spectrosc.* 2005;47(3–4):123–36.
34. van Wüllen L, Tricot G, Wegner S. An advanced NMR protocol for the structural characterization of aluminophosphate glasses. *Solid State Nucl Magn Reson.* 2007;32(2):44–52.
35. Gullion T. Introduction to rotational-echo, double-resonance NMR. *Concepts Magn Reson.* 1998;10(5):277–89.
36. Gullion T, Schaefer J. Rotational-echo double-resonance NMR. *J Magn Reson.* 1989;81(1):196–200.
37. Pan Y, Gullion T, Schaefer J. Determination of C-N internuclear distances by rotational-echo double-resonance NMR of solids. *J Magn Reson.* 1990;90(2):330–40.
38. Limbach R, Karlsson S, Scannell G, Mathew R, Edén M, Wondraczek L. The effect of TiO_2 on the structure of $\text{Na}_2\text{O-CaO-SiO}_2$ glasses and its implications for thermal and mechanical properties. *J Non-Cryst Solids.* 2017;471:6–18.
39. Griebenow K, Kamitsos EI, Wondraczek L. Mixed-modifier effect in (Ca, Mg) metaphosphate glasses. *J Non-Cryst Solids.* 2017;468:74–81.
40. Möncke D, Ehrt D, Velli LL, Varsamis C, Kamitsos EI. Structure and properties of mixed phosphate and fluoride glasses. *Phys Chem Glasses.* 2005;46(2):67–71.
41. Brow RK, Tallant DR, Hudgens JJ, Martin SW, Irwin AD. The short-range structure of sodium ultraphosphate glasses. *J Non-Cryst Solids.* 1994;177:221–8.

42. Nelson BN, Exarhos GJ. Vibrational spectroscopy of cation-site interactions in phosphate glasses. *J Chem Phys.* 1979;71(7):2739–47.
43. Velli LL, Varsamis C, Kamitsos EI, Möncke D, Ehrt D. Structural investigation of metaphosphate glasses. *Phys Chem Glasses.* 2005;46(2):178–81.
44. Konidakis I, Varsamis C, Kamitsos EI, Möncke D, Ehrt D. Structure and properties of mixed Strontium-Manganese metaphosphate glasses. *J Phys Chem C.* 2010;114(19):9125–38.
45. Kamitsos EI, Kapoutsis JA, Chrysos GD, Hutchinson JM, Pappin AJ, Ingram MD, et al. Infrared study of AgI containing superionic glasses. *Phys Chem Glasses.* 1995;36(3):141–9.
46. Möncke D, Neto M, Bradtmüller H, de Souza GB, Rodrigues AM, Elkholy HS, et al. $\text{NaPO}_3\text{-AlF}_3$ glasses: Fluorine evaporation during melting and the resulting variations in structure and properties. *J Chem Technol Metall.* 2018;53(6):1047–60.
47. Brow RK, Tallant DR. Structural design of sealing glasses. *J Non-Cryst Solids.* 1997;222:396–406.
48. Plotnichenko VG, Sokolov VO, Koltashev VV, Dianov EM. On the structure of phosphosilicate glasses. *J Non-Cryst Solids.* 2002;306(3):209–26.
49. Chakraborty IN, Condrate RA. The vibrational spectra of glasses in the $\text{Na}_2\text{O-SiO}_2\text{-P}_2\text{O}_5$ system with a 1:1 $\text{SiO}_2\text{:P}_2\text{O}_5$ molar ratio. *Phys Chem Glasses.* 1985;26(3):68–73.
50. Belkebir A, Rocha J, Esculcas AP, Berthet P, Gilbert B, Gabelica Z, et al. Structural characterisation of glassy phases in the system $\text{Na}_2\text{O-Al}_2\text{O}_3\text{-P}_2\text{O}_5$ by MAS and solution NMR, EXAFS and vibrational spectroscopy. *Spectrochim Acta Mol Biomol Spectros.* 1999;55(7–8):1323–36.
51. Le QH, Palenta T, Benzine O, Griebenow K, Limbach R, Kamitsos EI, et al. Formation, structure and properties of fluoro-sulfo-phosphate poly-anionic glasses. *J Non-Cryst Solids.* 2017;477(Supplement C):58–72.
52. Wong J, Angell CA. *Glass: structure by spectroscopy.* New York: Marcel Dekker; 1976.
53. Chakraborty IN, Condrate RA, Ferraro JR, Chenuit CF. The vibrational spectra and normal coordinate analyses of cubic and monoclinic SiP_2O_7 . *J Solid State Chem.* 1987;68(1):94–105.
54. Kamitsos EI, Risen WM. Vibrational spectra of single and mixed alkali pentasilicate glasses. *J Non-Cryst Solids.* 1984;65:333.
55. Kamitsos EI, Kapoutsis JA, Jain H, Hsieh CH. Vibrational study of the role of trivalent ions in sodium trisilicate glass. *J Non-Cryst Solids.* 1994;171:31.
56. Kamitsos EI, Chrysos GD. Alkali sites in glass. *Solid State Ionics.* 1998;105(1–4):75–85.
57. Wegner S, van Wüllen L, Tricot G. The structure of aluminophosphate glasses revisited: Application of modern solid state NMR strategies to determine structural motifs on intermediate length scales. *J Non-Cryst Solids.* 2008;354(15–16):1703–14.
58. Massiot D, Fayon F, Capron M, King I, Le Calvé S, Alonso B, et al. Modelling one- and two-dimensional solid-state NMR spectra. *Magn Reson Chem.* 2002;40(1):70–6.
59. Ren JJ, Eckert H. Superstructural units involving six-coordinated silicon in sodium phosphosilicate glasses detected by solid-state NMR spectroscopy. *J Phys Chem C.* 2018;122(48):27620–30.
60. Limbach R, Rodrigues BP, Möncke D, Wondraczek L. Elasticity, deformation and fracture of mixed fluoride-phosphate glasses. *J Non-Cryst Solids.* 2015;430:99–107.
61. Benzine O, Bruns S, Pan Z, Durst K, Wondraczek L. Local deformation of glasses is mediated by rigidity fluctuation on nanometer scale. *Adv Sci.* 2018;5(10):1800916.
62. Rouxel T. Elastic properties and short-to medium-range order in glasses. *J Am Ceram Soc.* 2007;90(10):3019–39.

SUPPORTING INFORMATION

Additional supporting information may be found online in the Supporting Information section.

How to cite this article: Sawangboon N, Nizamutdinova A, Uesbeck T, et al. Modification of silicophosphate glass composition, structure, and properties via crucible material and melting conditions. *Int J Appl Glass Sci.* 2020;11:46–57. <https://doi.org/10.1111/ijag.13958>